2013

A Single-Parameter Model of the Immune Response to Bacterial Invasion

Lester Caudill
University of Richmond, lcaudill@richmond.edu

A Single-Parameter Model of the Immune Response to Bacterial Invasion

Lester F. Caudill, Jr.

Department of Mathematics and Computer Science, University of Richmond, Richmond, VA 23173, USA

Abstract The human immune response to bacterial pathogens is a remarkably complex process, involving many different cell types, chemical signals, and extensive lines of communication. Mathematical models of this system have become increasingly high-dimensional and complicated, as researchers seek to capture many of the major dynamics. In this paper, we argue that, in some important instances, preference should be given to low-dimensional models of immune response, as opposed to their high-dimensional counterparts. One such model is analyzed and shown to reflect many of the key phenomenological properties of the immune response in humans. Notably, this model includes a single parameter that, when combined with a single set of reference parameter values, may be used to quantify the overall immunocompetence of individual hosts.

Key words immune response · mathematical model · differential equations model · stability analysis · similarity parameter

1. Introduction

A healthy human body responds to invasion by non-resident bacteria through a complex and well-orchestrated cascade of physical and biochemical events and processes, collectively referred to as the *immune response* [**?**]. Such a response by the host's immune system to bacterial invasion can only end in one of three possible ways [**?**]:

1. *Pathogen elimination.* The invading bacteria is fully-eliminated from the body of the host.

E-mail address: lcaudill@richmond.edu.

2. *Response failure.* The host's immune response fails to control the actions of the invading bacteria. This often leads to the death of the host.

3. *Endemicity.* The bacteria's growth is controlled (but not to the point of elimination), and its activities regulated. In this outcome, the invading bacteria is essentially incorporated into the host's resident microflora.

As in many other areas of human (and non-human) health, mathematical models of the immune response can play an important role in exploring potential strategies to prevent or control infections by bacterial pathogens. Models, and their implementation as computer simulation tools, can provide valuable insight, especially regarding questions whose empirical investigation is limited by time demands, expense, and potential danger to test subjects. One example, of particular interest to the author, involves the rise and spread of antibiotic resistance in bacterial pathogens, especially in hospital settings [**?**]. A number of control strategies for antibiotic resistance have been proposed in the medical community, but many still await investigation, due to associated cost and risk [**??**]. A useful mathematical model of this process, capable of incorporating and testing proposed control strategies, must of necessity include, among many factors, the important impact of the immune response on the infection dynamics [**?**]. In this setting, where the immune response is to be included as one of several components in an overall host-pathogen interaction model, one must compromise between realism and manageability. Given the high level-of-complexity of the immune response, and the sheer number of different cells, proteins, and chemical signals involved, any mechanistic model (i.e. a model that seeks to simulate the dynamics of the underlying interactions between the different immune components and the pathogen) must of necessity be large and complex. Such models have proven useful in investigating some immune-related questions, but become unmanageable in settings such as the current one, where the immune response is but one of several (similarly complex) components which comprise the overall model. In such cases, one may look to lower-dimensional models that are considered more phenomenological, that is, they seek to accurately capture the overall effects of the immune response, without the level-of-detail of the mechanistic models.

The goal of the present work is to present the development and analysis of a low-dimensional phenomenological model of the immune response

to a replicating bacterial pathogen. The ideal would be a two-dimensional model, in which one dependent quantity represents the invading pathogen, and the other dependent quantity represents some proxy (e.g. antibodies) of immune system activity. The majority of existing immune response models are of the mechanistic type, involving large-dimensional model systems with many model parameters [**??????????????**]. Such models, while impressive in their level-of-detail, do not meet the needs of the present work. A smaller number of existing models may be considered more phenomenological, including a number of low-dimensional models. Many of these low-dimensional models can be viewed as extensions and improvements on the predator-prey-inspired models of Bell from the early-1970s [**?**]. It is reasonable to demand that, even for a low-dimensional model, all three possible outcomes (pathogen elimination, response failure, and endemicity) be realizable for achievable parameter values. However, to the author's knowledge, few published low-dimensional models can achieve all three. Bell's model [**?**] can lead to failure or endemicity, but never elimination. Huang's model [**?**] can only achieve all three outcomes in the unrealistic case in which the antibody population grows unboundedly. The model of Nowak, May, and Sigmund [**?**] predicts endemicity, but neither elimination nor failure. Nowak and Bangham [**?**] develop a four-dimensional model, which may be reduced to two dimensions, and can realize elimination and endemicity, but not failure. More recently, the work of Chaui-Berlinck, Marzagao, and Monteiro [**?**] features a model that can realize elimination and failure, but its ability to display endemicity is less-clear. By contrast, De Boer and Boerlijst [**?**] and Wodarz and Nowak [**?**] present models of immune response to a replicating pathogen that are two-dimensional and four-dimensional, respectively. While these models can realize all three possible outcomes, they are not suitable for the present needs, because their structure makes them applicable only to viral agents such as HIV.

As will be seen, the present model includes a total of eight parameters (seven of which are dependent, at least in part, on the competency of the host's immune response), a significant reduction from the parameter counts in the aforementioned mechanistic models, but still a large number, especially in the situation where multiple hosts, each with their own specific seven-parameter immunocompetencies, are considered. To improve this situation, we introduce a dimensionless similarity parameter (which we will refer to as the *IC-parameter*, λ) into our model. In this way, we realize the following advance in practicality: Given a single pathogen species, we first fix the

values of the original eight model parameters. Then, each host is assigned its own specific value for λ, reflecting that individual's immunocompetence (with a larger value indicating a stronger immune response). For each host, the relevant pathogen-immune dynamics are then modeled with the fixed reference parameter values, combined with that host's λ-value. Thus, for a single pathogen species, our model requires only the eight reference parameter values (regardless of the number of hosts), appended by one λ-value for each host (hence, the "single parameter" reference in the title), a significant reduction from the "eight parameter values per host" alternative.

The balance of this paper is organized as follows: In Section 2, our model is developed and presented, and the IC-parameter λ is incorporated. In Section 3, we state our main result, which establishes that our model is able, under mild conditions on the model parameters, to realize all three possible clinical outcomes (pathogen elimination, response failure, and endemicity), as the value of λ varies over its domain. Section 4 contains numerical demonstrations, while conclusions and final words comprise Section 5.

2. Immune Response Model

Our model consists of two initial-value problems, simulating the interactions of a population p of a species of bacterial pathogen with a population i of proxy cells (e.g. antibodies) for the immune response. The change in the pathogen population over time τ is modeled by

$$\frac{dp}{d\tau} = ap - \frac{bpi}{K+p}\,, \quad p(0) = p_0\,. \tag{1}$$

while the corresponding change in the proxy immune population is modeled by

$$\frac{di}{d\tau} = \frac{cp}{B+p} + \frac{di}{M+i} - qi\,, \quad i(0) = i_0\,, \tag{2}$$

The three terms on the right-hand side of the second equation represent immune system stimulation due to pathogen presence, additional immune stimulation due to auto-stimulation, and natural breakdown of immune responders, respectively. The two terms on the right-hand side of the first equation represent intrinsic growth of the pathogen population and the removal of pathogen by the immune responders, respectively.

In an effort to reduce the number of model parameters that must be assigned to each individual host, we introduce a dimensionless similarity parameter λ (called the *IC-parameter*), whose value will represent the overall immunocompetence of the host with respect to the specific pathogen, with a larger value representing a stronger (i.e. more-effective) immune response. Following the logic established by Zuev and collaborators [**???**], we introduce our IC-parameter via the mappings

- $p \mapsto \lambda^{-\frac{3}{2}} p\,, \;\; i \mapsto \lambda^{-\frac{3}{2}} i$
- $K \mapsto \lambda^{-\frac{3}{2}} K\,, \;\; B \mapsto \lambda^{-\frac{3}{2}} B\,, \;\; M \mapsto \lambda^{-\frac{3}{2}} M$
- $a \mapsto \dfrac{a}{\lambda}\,, \;\; b \mapsto \dfrac{b}{\lambda}\,, \;\; c \mapsto \dfrac{c}{\lambda}\,, \;\; d \mapsto \dfrac{d}{\lambda}\,, \;\; q \mapsto \dfrac{q}{\lambda}\,,$

resulting in the revised model

$$\frac{dp}{d\tau} = \frac{a}{\lambda} p - \frac{b}{\lambda} \frac{pi}{K+p}\,, \quad p(0) = p_0\,. \tag{3}$$

$$\frac{di}{d\tau} = \frac{\lambda^{\frac{1}{2}} cp}{B+p} + \frac{\lambda^{\frac{1}{2}} di}{M+i} - \frac{q}{\lambda} i\,, \quad i(0) = i_0\,. \tag{4}$$

The main result of this work addresses the long-term behavior of solutions of (3)-(4), as λ progresses through a range of positive values.

Given that the IVP system (3)-(4) is intended to model the interaction of two physical populations, it is important to verify that solutions of this system cannot become negative.

Theorem 1 *If $p_0 > 0$ and $i_0 > 0$, then the solution $(p(\tau), i(\tau))$ of the IVP system (3)-(4) must satisfy $p(\tau) > 0$ and $i(\tau) > 0$ for every $\tau > 0$.*

Proof. Assume (by way of contradiction) that either $p(\tau) \leq 0$ or $i(\tau) \leq 0$ for some $\tau > 0$. Then, there exists a first τ-value, τ_0, for which $p(\tau_0) i(\tau_0) = 0$. Then, since $p(\tau) \geq 0$ and $i(\tau) \geq 0$ for $0 \leq \tau \leq \tau_0$, the functions

$$\psi_p(\tau) \equiv \frac{a}{\lambda} - \frac{b}{\lambda} \frac{i(\tau)}{K + p(\tau)} \qquad \text{and} \qquad \psi_i(\tau) \equiv \frac{\lambda^{\frac{1}{2}} d}{M + i(\tau)} - \frac{q}{\lambda}$$

are both continuous on $0 \leq \tau \leq \tau_0$, and have finite absolute minima M_p and M_i, on this interval. So,

$$\frac{dp}{d\tau} = \frac{a}{\lambda}p - \frac{b}{\lambda}\frac{pi}{K+p} = \psi_p(\tau)p \geq M_p p,$$

and

$$\frac{di}{d\tau} = \frac{\lambda^{\frac{1}{2}}cp}{B+p} + \frac{\lambda^{\frac{1}{2}}di}{M+i} - \frac{q}{\lambda}i = \frac{\lambda^{\frac{1}{2}}cp}{B+p} + \psi_i(\tau)i \geq M_i i\,.$$

Consequently, the Mean Value Theorem yields

$$p(\tau_0) \geq p_0 e^{M_p \tau_0} > 0 \qquad \text{and} \qquad i(\tau_0) \geq i_0 e^{M_i \tau_0} > 0\,,$$

which contradicts the assumption that $p(\tau_0)i(\tau_0) = 0$. Thus, $p(\tau) > 0$ and $i(\tau) > 0$ for every $\tau > 0$. □

3. Main Result

The main result of this work is the following:

Theorem 2 *Let a, b, c, d, q, B, K, $M > 0$. If $\dfrac{adB}{bcM}\left(\dfrac{K}{B} - 1\right) < 1$, then there exist constants L_1 and L_2, with $0 < L_1 < L_2$ such that*

- $0 < \lambda < L_1 \Rightarrow$ *system (3)-(4) has no stable equilibrium, and* $\lim_{\tau\to\infty} p(\tau) = +\infty$.
- $L_1 < \lambda < L_2 \Rightarrow$ *system (3)-(4) has a locally-stable endemic equilibrium.*
- $\lambda \geq L_2 \Rightarrow$ *system (3)-(4) has a locally-asymptotically-stable elimination (i.e. pathogen-free) equilibrium.*

Before presenting a proof of this result, we note that, by introducing the dimensionless variables $t = \dfrac{d}{K}\tau$, $P = \dfrac{p}{K}$, and $I = \dfrac{i}{M}$, the model system (3)-(4) can be rewritten as

$$\frac{dP}{dt} = \frac{\alpha}{\lambda}P - \frac{\beta}{\lambda}\left(\frac{PI}{1+P}\right), \quad P(0) = P_0\,, \tag{5}$$

$$\frac{dI}{dt} = \lambda^{\frac{1}{2}}\gamma\left(\frac{P}{1+\delta P}\right) + \frac{\lambda^{\frac{1}{2}}I}{1+I} - \frac{\phi}{\lambda}I\,, \quad I(0) = I_0 \tag{6}$$

where

$$\alpha = \frac{aM}{d},\ \beta = \frac{bM^2}{dK},\ \gamma = \frac{cK}{dB},\ \delta = \frac{K}{B},\ \phi = \frac{qM}{d},\ P_0 = \frac{p_0}{K},\ \text{ and }\ I_0 = \frac{i_0}{M}\,.$$

The proof of Theorem 2 begins with an analysis of the nullclines of (5)-(6). The P-nullclines are the straight lines

$$P = 0 \quad \text{and} \quad P_R(I) = \frac{\beta}{\alpha}I - 1\,,$$

while the I-nullclines are the curves that constitute the plot of the function

$$P_G(I) = \frac{\sigma_\lambda(I)}{\gamma - \delta\sigma_\lambda(I)}\,, \tag{7}$$

where

$$\sigma_\lambda(I) \equiv \phi\lambda^{-\frac{3}{2}}I - \frac{I}{1+I}\,. \tag{8}$$

In the next result, we collect some facts about the function $P_G(I)$ that will aid in visualizing these I-nullclines. These facts are self-evident from the formula (7), and are stated without proof.

Lemma 1 *The function $P_G(I)$ defined by (7) has the following properties:*

- *Roots at $I = 0$ and $I = \dfrac{\lambda^{\frac{3}{2}}}{\phi} - 1$.*

- *Vertical asymptotes at the roots* $I_- < 0$ *and* $I_+ > 0$ *of the quadratic equation*

$$\phi I^2 + \left(\phi - \lambda^{\frac{3}{2}}\left(\frac{\gamma}{\delta} + 1\right)\right) I - \frac{\gamma}{\delta}\lambda^{\frac{3}{2}} = 0\,. \tag{9}$$

- *A removable singularity at* $I = -1$.

- $\lim_{I \to \pm\infty} P_G(I) = -\frac{1}{\delta}\,.$

- $P_G'(I) \begin{cases} < 0, & -\sqrt{\frac{\lambda^{\frac{3}{2}}}{\phi}} - 1 < I < \sqrt{\frac{\lambda^{\frac{3}{2}}}{\phi}} - 1 \\ = 0, & I = -\sqrt{\frac{\lambda^{\frac{3}{2}}}{\phi}} - 1 \text{ or } \sqrt{\frac{\lambda^{\frac{3}{2}}}{\phi}} - 1 \\ > 0, & I < -\sqrt{\frac{\lambda^{\frac{3}{2}}}{\phi}} - 1 \text{ or } I > \sqrt{\frac{\lambda^{\frac{3}{2}}}{\phi}} - 1 \end{cases},$

Lemma 1 suggests three possible plots for $P_G(I)$ (See Fig. 1.), depending on the sign of $\frac{\lambda^{\frac{3}{2}}}{\phi} - 1$.

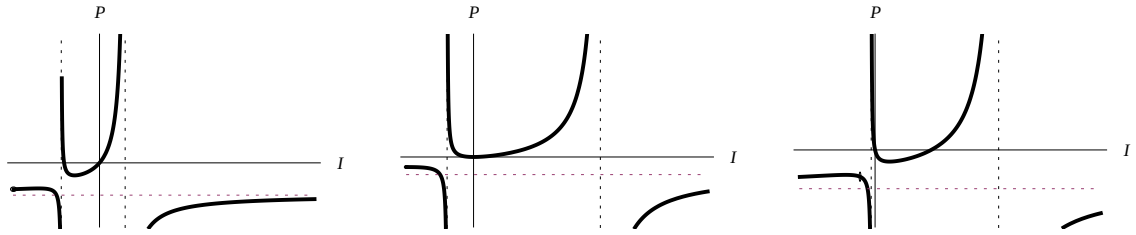

Fig.1 Three possible plots of $P_G(I)$, depending on whether $\frac{\lambda^{\frac{3}{2}}}{\phi} - 1$ is < 0 (left), $= 0$ (center), or > 0 (right).

Next, we investigate the sign distributions of $\frac{dP}{dt}$ and $\frac{dI}{dt}$. Beginning with $\frac{dP}{dt}$, we note that equation (5) can be rewritten as

$$\frac{dP}{dt} = \frac{\alpha}{\lambda} P \left(\frac{P - P_R(I)}{1 + P} \right) ,$$

which leads to the sign distribution for $\frac{dP}{dt}$ shown in Figure 2(a).

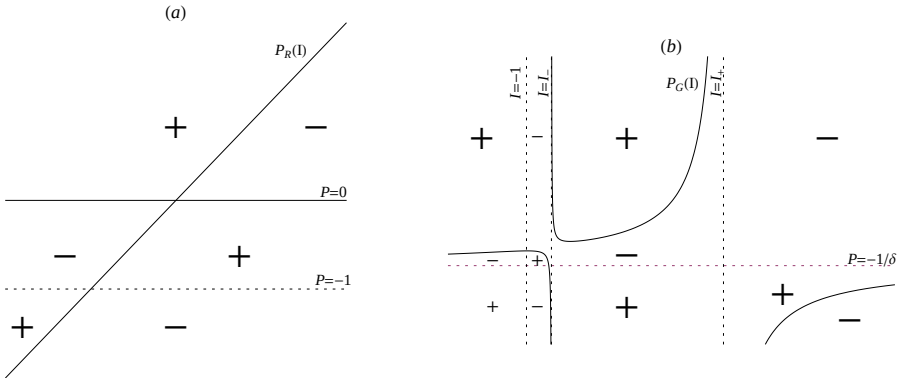

Fig.2 Sign distribution plot for $\frac{dP}{dt}$ (a) and for $\frac{dI}{dt}$ (b).

For $\frac{dI}{dt}$, note that, by utilizing (7), equation (6) can be rewritten as

$$\frac{dI}{dt} = \frac{\lambda^{\frac{1}{2}}(P - P_G(I))(\gamma - \delta\sigma_\lambda(I))}{1 + \delta P} . \tag{10}$$

Further, it follows from the definition (8) that

$$\gamma - \delta\sigma_\lambda(I) = \frac{-\delta \left(\phi I^2 + \left(\phi - \lambda^{\frac{3}{2}} \left(\frac{\gamma}{\delta} + 1 \right) \right) I - \frac{\gamma}{\delta} \lambda^{\frac{3}{2}} \right)}{\lambda^{\frac{3}{2}}(1 + I)} ,$$

which, in turn, factors into

$$\gamma - \delta\sigma_\lambda(I) = \frac{-\delta\phi(I - I_-)(I - I_+)}{\lambda^{\frac{3}{2}}(1 + I)} ,$$

where I_- and I_+ are the roots of equation (9). Combining this with (10) yields

$$\frac{dI}{dt} = \frac{-\delta\phi(P - P_G(I))(I - I_-)(I - I_+)}{\lambda(1 + \delta P)(1 + I)} ,$$

which leads to the sign distribution for $\dfrac{dI}{dt}$ shown in Figure 2(b).

At this point, to keep things manageable, we restrict our focus to the first quadrant. In doing so, we obtain the sign distributions shown in Figure 3.

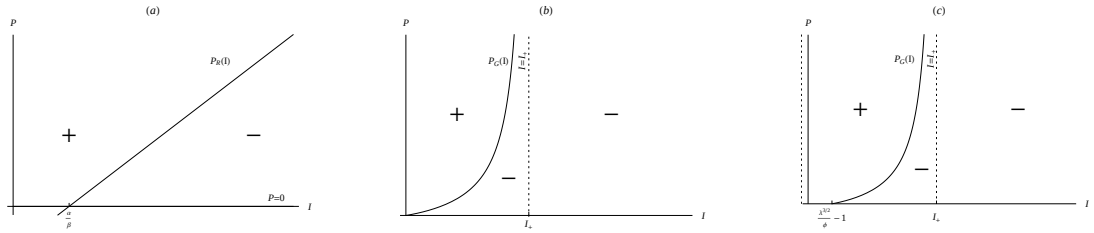

Fig.3 First-quadrant sign distribution plots: (a) $\dfrac{dP}{dt}$, (b) $\dfrac{dI}{dt}$ when $\dfrac{\lambda^{\frac{3}{2}}}{\phi} - 1 \leq 0$, and ($c$) $\dfrac{dI}{dt}$ when $\dfrac{\lambda^{\frac{3}{2}}}{\phi} - 1 > 0$.

We will utilize these sign distributions in the sequel, to derive phase-plane diagrams of (5)-(6) as needed.

We now investigate conditions under which the conclusion of Theorem 2 holds. We begin by considering how the phase-plane diagram of (5)-(6) varies with λ. It is convenient to first consider the case where $\lambda = \phi^{\frac{2}{3}}$. The key result in this case is the following.

Theorem 3 *Consider (5)-(6) with $\lambda = \phi^{\frac{2}{3}}$. There exists $\epsilon > 0$ such that, if $\dfrac{\alpha}{\beta} < \epsilon$, then (5)-(6) possesses exactly two equilibrium solutions (I_1, P_1) and (I_2, P_2) for which $0 < I_1 < I_2 < I_+$ and $P_1, P_2 > 0$.*

The proof of this result is facilitated by the following lemma:

Lemma 2 *For $\dfrac{\alpha}{\beta}$ sufficiently small, the cubic polynomial*

$$\hat{Q}(I) = \delta I^3 - \frac{\alpha}{\beta}(\delta - 1)I^2 - \gamma I$$

has exactly one root in the interval $0 < I < I_+$.

Proof. The fact that $\hat{Q}(I)$ has exactly one positive root follows from $\delta > 0$, $\hat{Q}(0) = 0$, and $\hat{Q}'(0) < 0$. Moreover, this positive root (which we denote by ρ) is given by

$$\rho \equiv \frac{\frac{\alpha}{\beta}(\delta - 1) + \sqrt{\frac{\alpha^2}{\beta^2}(\delta - 1)^2 + 4\gamma\delta}}{2\delta} \,.$$

Setting $\lambda = \phi^{\frac{2}{3}}$ in (9), we obtain an explicit expression for I_+:

$$I_+ = \frac{\gamma + \sqrt{\gamma^2 + 4\gamma\delta}}{2\delta} \,.$$

By virtue of the fact that the function

$$F(x) \equiv \frac{x + \sqrt{x^2 + 4\gamma\delta}}{2\delta}$$

is strictly increasing for all x, we see that, by choosing $\dfrac{\alpha}{\beta}$ so that $\dfrac{\alpha}{\beta}(\delta - 1) < \gamma$, we have

$$F\left(\frac{\alpha}{\beta}(\delta - 1)\right) < F(\gamma) \,,$$

so that

$$\rho < I_+ \,.$$

So, $\rho \in (0, I_+)$. □

We now proceed to a proof of Theorem 3:
Proof. We show that the equation

$$P_G(I) = P_R(I) \tag{11}$$

has exactly two solutions in the interval $(0, I_+)$. Setting $\lambda = \phi^{\frac{2}{3}}$ in equation (7), equation (11) has the same positive solutions as the cubic equation

$$Q(I) \equiv \hat{Q}(I) + \gamma\frac{\alpha}{\beta} = 0 \,,$$

where $\hat{Q}(I)$ is the cubic from Lemma 2. From Lemma 2, we know that $\hat{Q}(I)$ has roots at $I = 0$ and $I = \rho$, and that $\rho \in (0, I_+)$ if $\dfrac{\alpha}{\beta}(\delta - 1) < \gamma$. A simple

continuity argument yields the existence of an $\epsilon_0 > 0$ such that, if $\dfrac{\alpha}{\beta} < \epsilon_0$, then $Q(I)$ has two distinct roots inside the interval $0 < I < I_+$. The proof is completed by taking $\epsilon = \min\left\{\dfrac{\gamma}{|\delta - 1|}\,,\, \epsilon_0\right\}$, and noting that $P_G(I) > 0$ for every $I \in (0, I_+)$. □

Combining Theorem 3 with the sign distributions in Figures 3(a) and 3(b), we obtain the phase-plane diagram, for $\lambda = \phi^{\frac{2}{3}}$, when $\dfrac{\alpha}{\beta}$ is sufficiently small, shown in Figure 4(a). It is evident that (I_1, P_1) is a locally-stable endemic equilibrium, while the remaining equilibria are unstable.

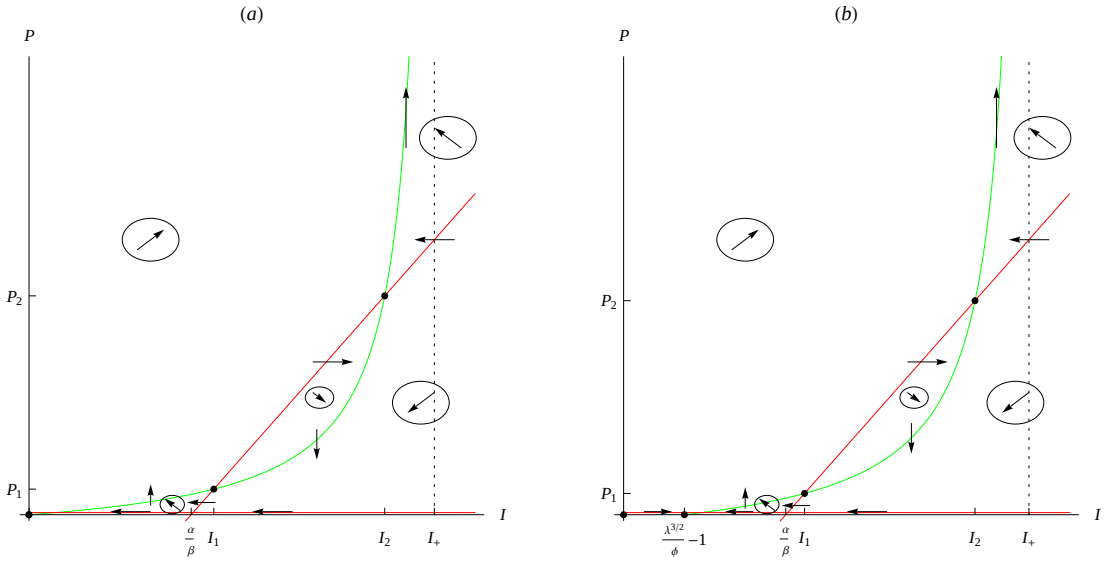

Fig.4 Phase-plane diagrams for the system (5)-(6), when $\lambda = \phi^{\frac{2}{3}}$ (a) and when $\phi^{\frac{2}{3}} < \lambda < \left(1 + \dfrac{\alpha}{\beta}\right)^{\frac{2}{3}} \phi^{\frac{2}{3}}$ (b). Circled arrows indicate direction of solution curves, with increasing t, in each sector.

As the value of λ is increased from $\phi^{\frac{2}{3}}$, the qualitative structure of the phase-plane diagram remains the same as in the $\lambda = \phi^{\frac{2}{3}}$ case, with the excep-

tion of the emergence of an additional (unstable) equilibrium at $\left(\frac{\lambda^{\frac{3}{2}}}{\phi} - 1, 0\right)$. (See Figure 4($b$).) This holds until $\lambda = \left(1 + \frac{\alpha}{\beta}\right)^{\frac{2}{3}} \phi^{\frac{2}{3}}$, at which point the equilibrium (I_1, P_1) merges with the equilibrium $\left(\frac{\lambda^{\frac{3}{2}}}{\phi} - 1, 0\right)$, and the phase-plane diagram takes the shape shown in Figure 5(a).

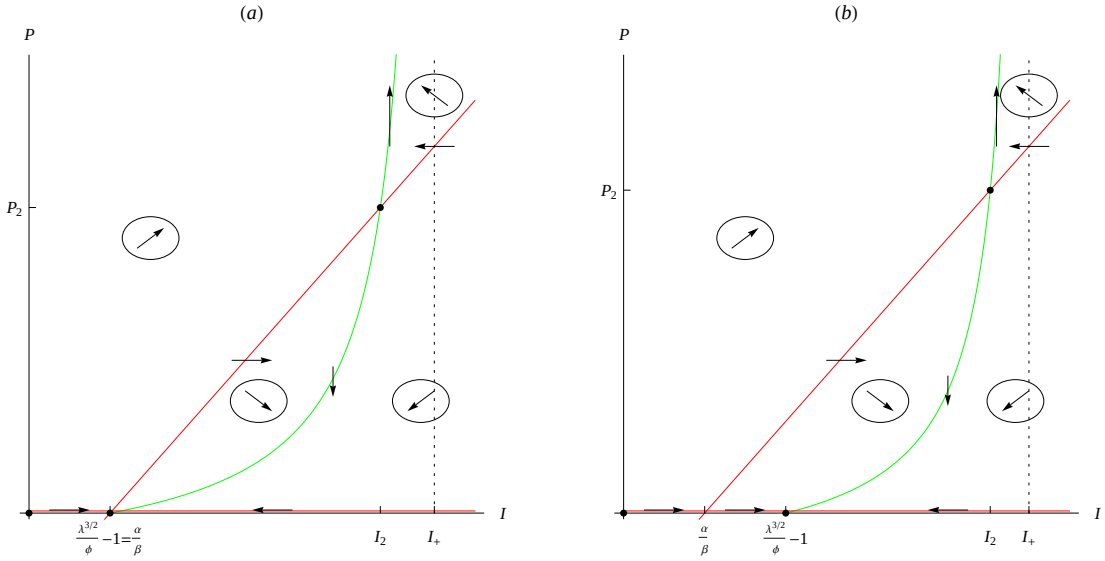

Fig.5 Phase-plane diagrams for the system (5)-(6), when $\lambda = \left(1 + \frac{\alpha}{\beta}\right)^{\frac{2}{3}} \phi^{\frac{2}{3}}$ (a) and when $\lambda > \left(1 + \frac{\alpha}{\beta}\right)^{\frac{2}{3}} \phi^{\frac{2}{3}}$ (b). Circled arrows indicate direction of solution curves, with increasing t, in each sector.

At this value of λ, the equilibrium $\left(\frac{\lambda^{\frac{3}{2}}}{\phi} - 1, 0\right)$ becomes locally-asymptotically stable, a property that it retains as λ is increased further. (See Figure 5(b).)

As the value of λ is decreased a small amount from $\phi^{\frac{2}{3}}$, the qualitative structure of the phase-plane diagram, as illustrated in Figure 4(a), is retained,

until a critical value $\lambda = \mu$, is reached, at which point the equilibrium (I_1, P_1) gets absorbed into (I_2, P_2), as illustrated in Figure 6(b). As a result, no stable equilibria remain.The existence of this critical number μ follows from the fact (which, in turn, follows from equation (9)) that

$$\lim_{\lambda \searrow 0} I_+ = 0\,.$$

Consequently, there exists an $\epsilon > 0$ for which $\lambda < \epsilon$ implies $I_+ < \dfrac{\alpha}{\beta}$. Since $P_G(I)$ exists (in the first quadrant) only for $0 \leq I < I_+$, it follows that $P_G(I)$ and $P_R(I)$ cannot intersect in this interval. So, no endemic equilibrium exists when $0 < \lambda < \epsilon$. A continuity argument then guarantees the existence of a unique $\mu > 0$ for which there is exactly one solution of equation (11) in the interval $0 \leq I < I_+$.

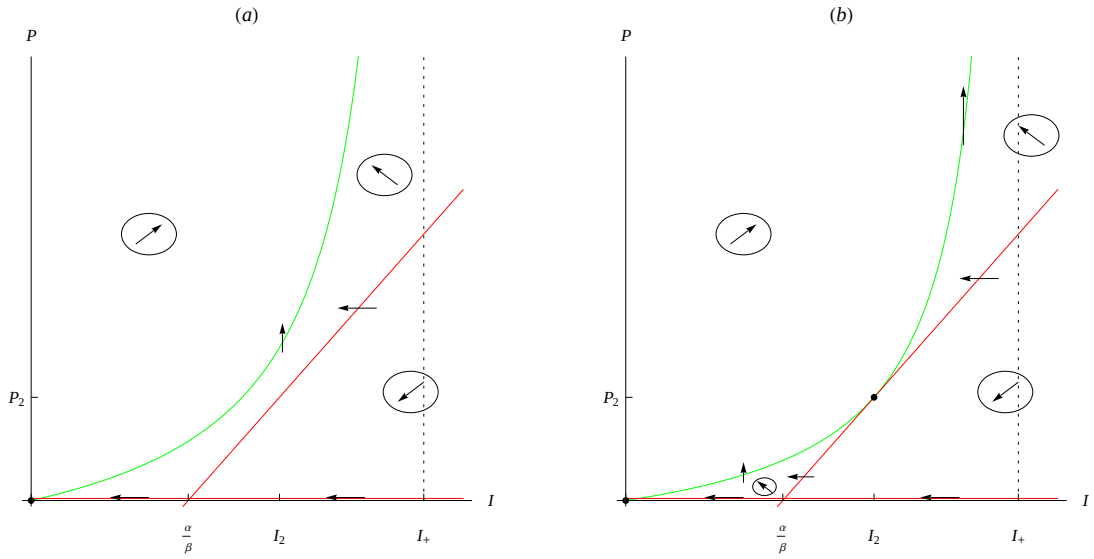

Fig.6 Phase-plane diagrams for the system (5)-(6), when $0 < \lambda < \mu$ (a) and when $\lambda = \mu$ (b). Circled arrows indicate direction of solution curves, with increasing t, in each sector.

Finally, for $0 < \lambda < \mu$, the phase-plane diagram takes the form shown in

Figure 6(a).

Now, we are prepared to complete the proof of Theorem 2.

Proof. Considering the preceding analysis, the proof is completed by setting $L_1 = \mu$ (the λ-value corresponding to Figure 6(b)) and $L_2 = \left(1 + \frac{\alpha}{\beta}\right)^{\frac{2}{3}} \phi^{\frac{2}{3}}$. □

Taken collectively, the phase-plane diagrams in Figures 4-6 suggest a bifurcation diagram of the form shown in Figure 7, which illustrates the following: As λ increases from 0, no stable equilibrium exists (and $P(t)$ grows unboundedly), until λ reaches μ, when a locally-stable endemic equilibrium appears. This continues through the bifurcation value at $\lambda = \phi^{\frac{2}{3}}$ as λ is increased further, until it reaches the third bifurcation value at $\left(1 + \frac{\alpha}{\beta}\right)^{\frac{2}{3}} \phi^{\frac{2}{3}}$, at which point the locally-stable endemic equilibrium is replaced by a locally-asymptotically-stable elimination equilibrium. Thus, as λ increases, we pass through the three possible outcomes delineated in the introduction: response failure, endemicity, and pathogen elimination.

4. Numerical Host Comparisons

We continue our investigation of the properties of the immune response model (5)-(6), and especially, the effects of differing values of the IC-parameter λ, through a number of multiple-host numerical comparisons. The first scenario compares three hosts, each of which has the same base parameter values (See the caption to Figure 8.) with respect to the pathogen in question, but with differing λ-values: For Host 1, $\lambda = 0.5$, for Host 2, $\lambda = 1$, and for Host 3, $\lambda = 2$. Each of these hosts experiences an initial invasion (so $I_0 = 0$ for each) by the same pathogen strain, and at the same level (i.e. the same value for P_0 in each case) but with different outcomes. Host 1, with the smallest λ-value, experiences failure of its immune response to control the pathogen, while Host 3, with the largest λ-value, is able to eliminate the pathogen. The immune response of Host 2, with the intermediate λ-value, can only achieve endemicity of the pathogen. These results, illustrated in Figure 8, demonstrate the ability of the model (5)-(6), with a single set of base parameter values, to reproduce each of the three possible outcomes of

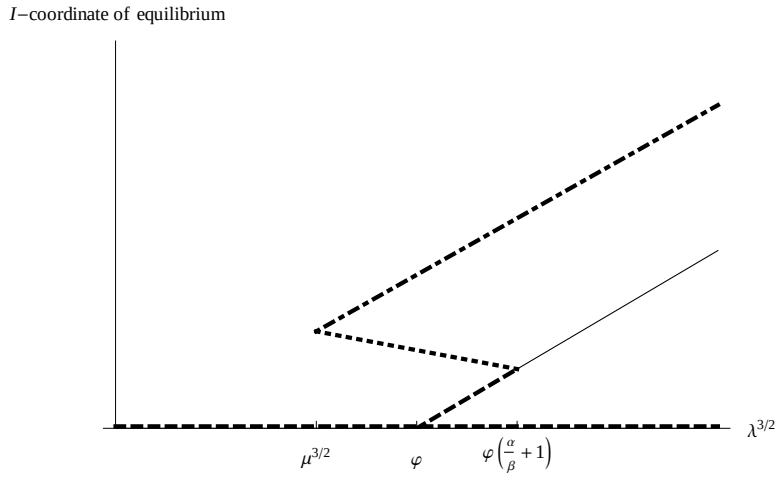

Fig.7 Bifurcation diagram, plotting the I-coordinate of the equilibria vs. the value of $\lambda^{\frac{3}{2}}$. The dashed line indicates unstable elimination equilibria, the dotted line indicates locally-stable endemic equilibria, the dot-dashed line indicates unstable endemic equilibria, and the solid line indicates locally-asymptotically-stable elimination equilibria.

bacteria-immune interaction (failure, endemicity, and elimination), simply by varying the value of the IC-parameter λ.

The second scenario is designed to explore the phenomenon known as *immunologic memory*. It is known that, after initial exposure to a pathogen, the human body is able to mount a faster, stronger, and more-effective immune response upon subsequent re-exposure to this same pathogen. This is thought to be due to the development of some B-leukocytes into memory cells, whose activities permit the immune system to more-readily recognize and respond to the invader [**?**]. To test our model's ability to simulate this phenomenon, we utilize two hosts, each with the same base parameters with respect to the pathogen in question, and each with the same value for the IC-parameter λ. (See the caption to Figure 9.) Initially, Host 1 experiences invasion by a pathogen at initial level P_{01}, while Host 2 does not. The immune response of Host 1 is sufficient to eliminate the pathogen invaders, and

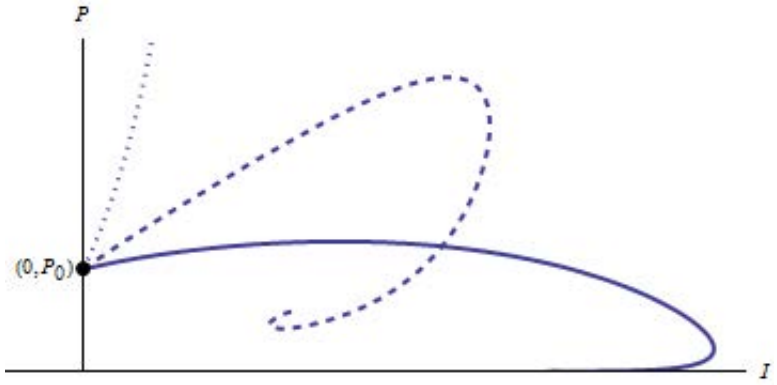

Fig.8 Model results from the three-host experiment, illustrating treatment failure for Host 1 ($\lambda = 0.5$, dotted), endemicity for Host 2 ($\lambda = 1$, dashed), and elimination for Host 3 ($\lambda = 2$, solid). Model parameter values used: $\alpha = 1$, $\beta = \frac{3}{2}$, $\phi = 1$, $\gamma = 2$, $\delta = 1$, $P_0 = 0.4$.

leaves Host 1 with a residual level I_{final} of immune proxies. Later, both Host 1 and Host 2 are exposed to the same pathogen, but at a larger initial level P_{02}, when compared to the first infection of Host 1. The fact that this is a second exposure in the case of Host 1, but a first exposure for Host 2, is evidenced in the different initial I-values for each. Because of this difference, Host 1 is able to clear the infection, while Host 2 is not, despite having identical model parameters, thereby demonstrating the impact of immunological memory in this instance. These results are illustrated in Figure 9.

5. Discussion

We have presented a two-equation, eight-parameter model of the phenomenological dynamics of interaction of a pathogen species with immune system proxies (e.g. antibodies) of a human host. We have incorporated an additional model parameter (the IC-parameter λ), to represent the overall immunocompetence of the host, and have demonstrated that, as the value of the IC-parameter increases, our model predicts a progression through the

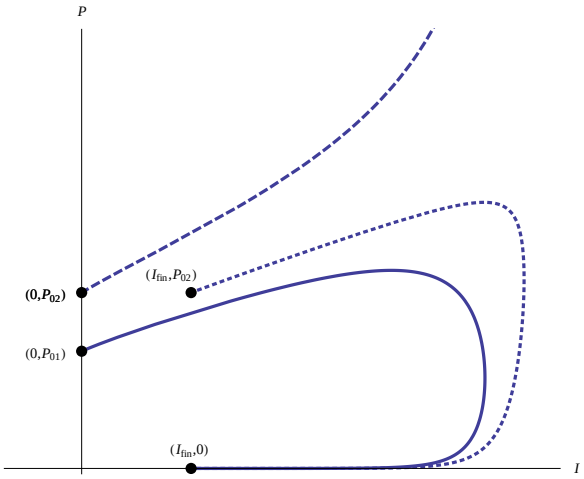

Fig.9 Model results from the two-host experiment. The solid curve shows the progression to elimination of Host 1's initial infection, while the dotted curve shows similar results from Host 1's second infection. By contrast, the initial infection of Host 2 (dashed curve) leads to treatment failure. Model parameter values used: $\alpha = 1$, $\beta = \frac{3}{2}$, $\phi = 1$, $\gamma = 2$, $\delta = 1$, $\lambda = 2$, $P_{01} = 4$, $P_{02} = 6$.

three possible clinical outcomes: from response failure through endemicity and, finally, pathogen elimination. Additionally, we have demonstrated, through numerical results, that our model reproduces the "immunologic memory," phenomenon, in which an initial pathogenic invasion, once eliminated, strengthens the host against future invasion by the same pathogen.

The principal advantage of the IC-parameter λ is to permit us to represent, with a single parameter, the overall effectiveness of the host's immune response to bacterial invasion. This advantage becomes evident in the case of multiple pathogens and multiple hosts, as we now demonstrate through a comparison of the extensions of model (1)-(2) and model (3)-(4) to the case of N pathogen species and H hosts. Noting that the N pathogen species give rise to N different populations of immune responders, each specific to one of the pathogen species, the model (1)-(2) extends naturally to the $2NH \times 2NH$ system

$$\frac{dp_{nj}}{d\tau} = a_{nj}p_{nj} - \frac{b_{nj}p_{nj}i_{nj}}{K_{nj} + p_{nj}}\,, \quad p_{nj}(0) = p_{nj,0}\,. \tag{12}$$

$$\frac{di_{nj}}{d\tau} = \frac{c_{nj}p_{nj}}{B_{nj} + p_{nj}} + \frac{d_{nj}i_{nj}}{M_{nj} + i_{nj}} - q_{nj}i_{nj}\,, \quad i(0) = i_{nj,0}\,, \tag{13}$$

for $n = 1, \ldots, N$ and $j = 1, \ldots, H$. Here, p_{nj} and i_{nj} indicate the pathogen load and the corresponding immune responder population, respectively, for pathogen n within host j. With this model, the eight model parameters must account not only for differences between pathogen species, but also differences in the immune system capabilities between the different hosts. Consequently, a total of $8NH$ different parameters are required for this model system. By contrast, the multi-pathogen, multi-host extension of (3)-(4):

$$\frac{dp_{nj}}{d\tau} = \frac{a_n}{\lambda_j}p_{nj} - \frac{b_n}{\lambda_j}\frac{p_{nj}i_{nj}}{K_n + p_{nj}}\,, \quad p_{nj}(0) = p_{nj,0}\,. \tag{14}$$

$$\frac{di_{nj}}{d\tau} = \frac{\lambda_j^{\frac{1}{2}}c_n p_{nj}}{B_n + p_{nj}} + \frac{\lambda_j^{\frac{1}{2}}d_n i_{nj}}{M_n + i_{nj}} - \frac{q_n}{\lambda_j}i_{nj}\,, \quad i_{nj}(0) = i_{nj,0}\,. \tag{15}$$

permits separation of the pathogen-dependent characteristics (embodied in the eight parameters a_n, b_n, K_n, c_n, B_n, d_n, M_n, and q_n) from the host-dependent characteristics (the IC-parameter λ_j). In this setting, modeling N pathogen species and H hosts requires only $8N + H$ different parameters. So, even a modest simulation involving, say, 12 hosts (a typical size − eight patients and four health-care workers − for a hospital intensive-care unit) and five pathogens, incorporating the IC-parameter will reduce the number of model parameters by nearly 90%, from 480 to 52. This significant reduction in model complexity will permit the inclusion of other factors, including antibiotic effects and host-host interactions, without rendering the model too complicated to be useful. Additionally, by incorporating this model into a larger model of infection dynamics [**?**], this ability to assign each host a single IC-parameter-value will permit investigation of the potential roles that immunodeficiency may play in small-population infection dynamics, including the rise and spread of antibiotic-resistant bacteria strains, where it has been conjectured that immunodeficient individuals may serve as reservoirs for antibiotic-resistant pathogens [**?**].

Acknowledgements

I am grateful to the University of Richmond for providing summer research support, and to Dr. Krista Stenger (Department of Biology, University of Richmond) for sharing her expertise in immunology.

References

R. Antia, C.T. Bergstrom, S.S. Pilyugin, S.M. Kaech, and R. Ahmed. Models of CD8+ responses: 1. What is the antigen-independent proliferation program. *J. Theor. Biol.*, 221(4):585–598, 2003.

A. Asachenkov, I. Pogozhev, and S. Zuev. Parametrization in mathematical models of immune-physiological processes. *Russ. J. Numer. Anal. Math. Modelling*, 8(1):31–46, 1993.

A. Asachenkov, G. Marchuk, R. Mohler, and S. Zuev. *Disease Dynamics.* Birkhauser, Boston, 1994.

K. Beck. A mathematical model of t-cell effects in the humoral immune response. *J. Theor. Biol.*, 89:593–610, 1981.

G.I. Bell. Predator-prey equations simulating an immune response. *Math. Biosci.*, 16:291–314, 1973.

R.J. De Boer and M.C. Boerlijst. Diversity and virulence thresholds in aids. *Proc. Natl. Acad. Sci. USA*, 94:544–548, 1994.

H.G. Boman. Innate immunity and the normal microflora. *Immunol. Rev.*, 173:5–16, 2000.

C. Bruni, M.A. Giovenco, G. Koch, and R. Strom. A dynamical model of humoral immune response. *Math. Biosci.*, 27:191–211, 1975.

L. Caudill and B. Lawson. A hybrid agent-based and differential equations model for simulating antibiotic resistance in a hospital ward. Technical Report TR-13-01, 2013. University of Richmond Mathematics and Computer Science.

J.G. Chaui-Berlinck, J.A.M. Barbuto, and L.H.A. Monteiro. Conditions for pathogen elimination by immune systems. *Theory Biosci.*, 123:195–208, 2004.

K.D. Elgert. *Immunology 2e*. Wiley-Blackwell, New York, 2009.

M.A. Fishman and A.S. Perelson. Modeling t cell-antigen presenting cell interactions. *J. Theor. Biol.*, 160:311–342, 1993.

D. Fouchet and R. Regoes. A population dynamics analysis of the interaction between adaptive regulatory t cells and antigen presenting cells. *PLoS ONE*, 3(5):e2306, 2008.

D.A. Goldmann, R.A. Weinstein, R.P. Wenzel, O.C. Tablan, R.J. Duma, R.P. Gaynes, J. Schlosser, and W.J. Martone. Strategies to prevent and control the emergence and spread of antimicrobial-resistant microorganisms in hospitals. *JAMA*, 275(3):234–240, 1996.

Z. Grossman, R. Asofsky, and C. DeLisi. The dynamics of antibody-secreting cell production: regulation of growth and oscillations in the response to t-independent antigen. *J. Theor. Biol.*, 84(1):49–92, 1980.

X.-C. Huang. Uniqueness of limit cycles in a predator-prey model simulating an immune response. In R. Mohler and A. Asachenkov, editors, *Selected Topics on Mathematical Models in Immunology and Medicine*, pages 147–153, Laxenburg, Austria, 1990. IIASA.

P. Klein and J. Dolezal. A mathematical model of antibody response dynamics. *Problems Control Inform. Theory*, 9:407–419, 1980.

H.Y. Lee, D.J. Topham, S.Y. Park, J. Hollenbaugh, J. Treanor, T.R. Mosmann, X. Jin, B.M. Ward, H. Miao, J. Holden-Wiltse, A.S. Perelson, M. Zand, and H. Wu. Simulation and prediction of the adaptive immune response to influenza a virus infection. *J. Virol.*, 83(14):7151–7165, 2009.

I. Mackay and F.S. Rosen. Advances in immunology. *N. Engl. J. Med.*, 343: 338–344, 2000.

G.I. Marchuk. *Mathematical Modeling of Immune Response in Infectious Diseases*. Kluwer, Boston, 1997.

A.R. McLean. Modeling t cell memory. *J. Theor. Biol.*, 170:63–74, 1994.

R. Moellering and H. Blumgart. Understanding antibiotic resistance development in the immunocompromised host. *Intl. J. Infect. Dis.*, 6:S3–S4, 2002.

R.R. Mohler, C.F. Barton, and C.-S. Hsu. T and b cells in the immune system. In G.I. Bell, A.S. Perelson, and G.H. Pimbley, editors, *Theoretical Immunology*, pages 415–435, New York, 1978. Marcel-Dekker.

M.A. Nowak and C.R.M. Bangham. Population dynamics of immune responses to persistent viruses. *Science, New Series*, 272(5258):74–79, 1996.

M.A. Nowak, R.M. May, and K. Sigmund. Immune responses against multiple epitopes. *J. Theor. Biol.*, 175:325–353, 1995.

I. Pogozhev, R. Usmanov, and S. Zuev. Models of processes in organism and population characteristics. *Russ. J. Numer. Anal. Math. Modelling*, 8(5): 441–452, 1993.

D. Prikrylova, M. Jilek, and J. Waniewski. *Mathematical Modeling of the Immune Response*. CRC Press, Boca Raton, FL, 1992.

A. Rundell, R. DeCarlo, H. HogenEsch, and P. Doerschuk. The humoral immune response hemophilus influenzae type : a mathematical model based on t-zone ad germinal center b-cell dynamics. *J. Theor. Biol.*, 194:341–381, 1998.

B. Spellberg, R. Guidos, D. Gilbert, J. Bradley, H.W. Boucher, W.M. Scheld, J.G. Bartlett, and J. Edwards. The epidemic of antibiotic-resistant infections: A call to action for the medical community from the infectious diseases society of america. *Clin. Infect. Dis.*, 46:155–164, 2008.

R. Usmanov and S. Zuev. Parametrization in mathematical models of diseases. *Russ. J. Numer. Anal. Math. Modelling*, 8(3):275–284, 1993.

P. Waltman. A threshold model of antigen-stimulated antibody production. In G.I. Bell, A.S. Perelson, and G.H. Pimbley, editors, *Theoretical Immunology*, pages 437–453, New York, 1978. Marcel-Dekker.

R.G. Weinand and M. Conrad. Maturation of the immune response: A computational model. *J. Theor. Biol.*, 133:409–428, 1988.